JACS
JOURNAL OF THE AMERICAN CHEMICAL SOCIETY
Communication
pubs.acs.org/JACS

Dye Regeneration Kinetics in Dye-Sensitized Solar Cells

Torben Daeneke,[†,‡] Attila J. Mozer,[§] Yu Uemura,[∥,⊥] Satoshi Makuta,[#] Monika Fekete,[†] Yasuhiro Tachibana,[#] Nagatoshi Koumura,[∥,⊥] Udo Bach,[*,‡,▽] and Leone Spiccia[*,†]

[†]School of Chemistry and ARC Centre of Excellence for Electromaterials Science, Monash University, Victoria 3800, Australia

[‡]Materials Science and Engineering, CSIRO, Clayton South, Victoria 3169, Australia

[§]Intelligent Polymer Research Institute and ARC Centre of Excellence for Electromaterials Science, University of Wollongong, New South Wales 2522, Australia

[∥]Research Institute for Photovoltaic Technology, National Institute of Advanced Industrial Science and Technology, 1-1-1 Higashi, Tsukuba, Ibaraki 305-8565, Japan

[⊥]Graduate School of Pure and Applied Sciences, University of Tsukuba, 1-1-1 Tennoudai, Tsukuba, Ibaraki 305-8571, Japan

[#]School of Aerospace, Mechanical and Manufacturing Engineering, RMIT University, Bundoora, Victoria 3083, Australia

[▽]Department of Materials Engineering, Monash University, Victoria 3800, Australia

Supporting Information

ABSTRACT: The ideal driving force for dye regeneration is an important parameter for the design of efficient dye-sensitized solar cells. Here, nanosecond laser transient absorption spectroscopy was used to measure the rates of regeneration of six organic carbazole-based dyes by nine ferrocene derivatives whose redox potentials vary by 0.85 V, resulting in 54 different driving-force conditions. It was found that the reaction follows the behavior expected for the Marcus normal region for driving forces below 29 kJ mol^{-1} (ΔE = 0.30 V). Driving forces of 29−101 kJ mol^{-1} (ΔE = 0.30−1.05 V) resulted in similar reaction rates, indicating that dye regeneration is diffusion controlled. Quantitative dye regeneration (theoretical regeneration yield 99.9%) can be achieved with a driving force of 20−25 kJ mol^{-1} ($\Delta E \approx$ 0.20−0.25 V).

Dye-sensitized solar cells (DSCs) are under intense investigation because of their potential to achieve efficient conversion of sunlight into electricity at competitive costs.[1] In these photoelectrochemical devices, a wide-band-gap semiconductor (typically TiO_2) is sensitized by a dye, which under illumination injects an electron into the TiO_2 conduction band. The electron diffuses through the mesoporous semiconductor network to the anode and then passes through an external circuit to the cathode, where it reduces the electroactive electrolyte, which in turn regenerates the dye. Dye regeneration is a crucial step in this cycle, which must occur rapidly to avoid charge recombination between the photooxidized dye and the injected electron and minimize dye degradation. In a previous study, we showed that an insufficient driving force for dye regeneration results in a low open-circuit voltage (V_{oc}) and poor short-circuit current density (J_{sc}) due to fast recombination of the injected electrons and the photooxidized dye molecules.[2] Excessive regeneration driving force leads to lower V_{oc}, limiting the energy conversion efficiency. Hence, elucidation of the optimum driving force for dye regeneration is important for the design of DSCs with maximum efficiency.

In this work, we examined the dye regeneration kinetics for combinations of organic carbazole dyes and a family of ferrocene (Fc) derivatives[3] (Figure 1). The relationship we obtained will aid the design of more efficient DSCs and contribute to efforts devoted to the modeling of DSCs. Furthermore, the results are likely to impact studies of other photoelectrochemical devices where charge separation after photooxidation of a chromophore is followed by regeneration.

In traditional DSC designs, the electrolyte contains I_3^-/I^-, a two-electron redox couple that is used to regenerate the dye and facilitate charge transport between the electrodes. Although efficiencies of >11% have been achieved, the use of I_3^-/I^- has some significant drawbacks that have stimulated interest in new redox mediators.[5] Recent attempts to replace I_3^-/I^- have led to some remarkable achievements.[6] In fact, the highest DSC efficiency of 12.3% was achieved using a $[Co(bpy)_3]^{2+/3+}$ based electrolyte in conjunction with a Zn^{II} porphyrin/organic dye combination.[7] A key to the improved efficiency was the closer matching of the redox potentials of the electrolyte and dye, minimizing excessive driving force.

Since the V_{oc} of the DSC is limited by the difference between the quasi Fermi level of electrons in TiO_2 and the redox potential of the electrolyte, higher cell voltages can in principle be achieved by using a redox shuttle with a higher redox potential. However, a minimum driving force for dye regeneration must be provided to prevent recombination between the photooxidized dye and the injected electron (Figure 1) and to maintain high J_{sc}.

The driving force for dye regeneration, $-\Delta G$, is commonly estimated from data obtained by cyclic voltammetry (CV) according to eq 1,

$$-\Delta G = \nu e \Delta E = \nu e[E_{1/2}(D^+/D) - E_{1/2}(Fc^{deriv+}/Fc^{deriv})] \quad (1)$$

where $E_{1/2}(D^+/D)$ and $E_{1/2}(Fc^{deriv+}/Fc^{deriv})$ are the redox potentials of the dye and the Fc derivative, respectively, ΔE is

Received: June 5, 2012
Published: September 27, 2012

   dx.doi.org/10.1021/ja3054578 | J. Am. Chem. Soc. 2012, 134, 16925−16928

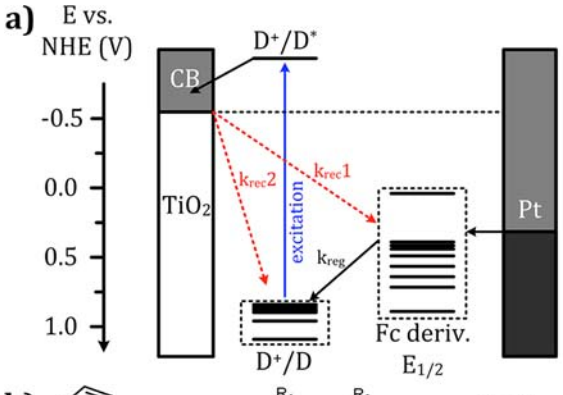

c)

Dye	n	m	R_1	R_2	R_3	$E_{1/2}$ vs. NHE (V)
MK 75	2	0	n-C_6H_{13}	--	CN	1.136
MK 1	3	0	n-C_6H_{13}	--	CN	0.948
MK 2	4	0	n-C_6H_{13}	--	CN	0.889
MK 24	4	0	n-C_3H_7	--	CN	0.883
MK 78	4	0	n-C_6H_{13}	--	H	0.882
MK 51	2	2	n-$C_4H_8OCH_3$	n-C_6H_{13}	CN	0.897

d)

Fc deriv.	$E_{1/2}$ vs. NHE (V)
$Me_{10}Fc$	0.088
Me_2Fc	0.504
Et_2Fc	0.497
i-Pr_2Fc	0.499
EtFc	0.555
Fc	0.620
$(Me_2Si)_2Fc$	0.671
BrFc	0.786
Br_2Fc	0.935

Figure 1. (a) Potential diagram of the DSC. (b) Structures of the dyes and ferrocene. (c) Redox potentials of the dyes. (d) Redox potentials of the ferrocene derivatives.[3] Redox potentials were measured by CV on 3 mM solutions (see the SI). The $E_{1/2}(D^+/D)$ potentials in (c) were measured after the dye was adsorbed on nanoporous ITO working electrodes. Potentials are reported in V vs NHE after conversion with $E_{1/2}(Fc) = 0.62$ V vs NHE.[4] The scan rate was 20 mV s^{-1}.

the potential difference between the dye and the Fc derivative, ν is the number of electrons transferred, and e is the elemental charge of the electron.[8]

To date, the effect of the driving force on the dye regeneration kinetics remains largely unknown. Previous studies have shown that the driving forces needed to achieve quantitative dye regeneration are higher for two-electron redox couples than for one-electron redox couples because their reaction mechanisms are more complex.[5b,9] By varying the redox potential of the sensitizer, Clifford et al.[10] showed that a dye with a regeneration driving force of 44 kJ mol^{-1} ($\Delta E = 0.46$ V) was not regenerated by iodide, whereas regeneration was efficient for a dye with a driving force of 68 kJ mol^{-1} ($\Delta E = 0.70$ V). A similar conclusion was reached in a comparison of I_3^-/I^- with pseudohalogens or thiolate/dithiol-based redox couples.[11] In general, one-electron redox couples appear to regenerate the dye efficiently when the driving force is larger than 35−38 kJ mol^{-1} ($\Delta E = 0.36$−0.39 V).[2,12] However, previous studies applying both one- and two-electron redox couples have varied either the dye or the redox couple but not both. As a result, no more than six different driving force conditions were covered in each study. Hence, it was difficult to elucidate fully the relationship between the dye regeneration rate constant, k_{reg}, and the driving force.

In this paper, we report k_{reg} values for the electron transfer between six ethylcarbazole-based donor−π-bridge−acceptor dyes and nine Fc derivatives (Figure 1). The energy levels of the dyes [adsorbed on nanoporous indium tin oxide (ITO) films] and the Fc derivatives were characterized by CV [Tables S1 and S2 in the Supporting Information (SI)]. The Fc derivatives[3] were ideal for this study since a redox potential range of 0.85 V (0.09 to 0.94 V vs NHE) was covered by substitution on one or both cyclopentadienyl rings. Similarly, the sensitizers covered a potential range of 0.26 V (0.88 to 1.14 V vs NHE). Here, the length of the conjugated oligothiophene unit significantly affected the redox potential, whereas changes in either the side chains (length, inclusion of ether groups) or the acceptor induced only small changes in the potential.

Dye regeneration rates were measured by means of nanosecond transient absorption spectroscopy (TAS)[13] using two different laser spectrometers to verify the results (see the SI for experimental details). In this experiment, a dye-sensitized TiO_2 film is excited by a nanosecond pulsed laser while in contact with an electrolyte solution. Photon absorption by the dye molecules results in electron injection into the TiO_2 film. A change in the electronic spectrum is observed that reflects the formation of the dye cation, consumption of ground-state dye (bleaching), a Stark shift of the dye absorption, and light absorption due to electrons in the TiO_2 conduction band.[14] Rate measurements were carried out by following the change in optical density (ΔOD) with time (t) at 900 nm, where the absorption of the dye cation is predominant.[15]

If the dye-sensitized film is in contact with an inert electrolyte devoid of the Fc derivative, the dye cation eventually recombines with the injected electrons. The recombination rate constant, k_{rec2}, can be determined from the absorbance−time profile. In the presence of the Fc derivative (reduced redox mediator), the dye cation can return to its ground state either by recombination or by reaction with the ferrocene (regeneration). The ΔOD versus t curve is typically modeled using a stretched exponential decay (eq 2),[13a] where $\Delta OD_{t=0}$ is the initial signal magnitude, τ_{ww} is the characteristic stretched lifetime, and β is the stretch parameter. The observed lifetime, τ_{obs}, and observed rate constant, k_{obs}, are calculated using eqs 3 and 4, where the Γ function in eq 3 is defined in eq 5. The value of k_{reg} is then calculated using eq 6 where $[Fc^{deriv}]$ is the Fc derivative concentration (5 mM in this work). (See ref 13a for more insight into eqs 2−6.)

$$\Delta OD(t) = \Delta OD_{t=0} e^{-(t/\tau_{ww})^{\beta}} \quad (2)$$

$$\tau_{obs} = \frac{\tau_{ww}}{\beta}\Gamma\left(\frac{1}{\beta}\right) \quad (3)$$

$$k_{obs} = \frac{1}{\tau_{obs}} \quad (4)$$

$$\Gamma(x) = \int_0^{\infty} u^{x-1} e^{-u}\, du \quad (5)$$

$$k_{reg} = \frac{k_{obs} - k_{rec2}}{[Fc^{deriv}]} \quad (6)$$

Figure 2 shows ΔOD versus t for MK1-sensitized TiO_2 films (data for the other dyes and the fitted parameter values can be found in Figures S1−S6 and Tables S3−S8 in the SI). The ΔOD versus t profiles clearly show that the rate of the dye regeneration reaction depends on the Fc derivative and, consequently, the driving force provided for the reaction.

dx.doi.org/10.1021/ja3054578 | J. Am. Chem. Soc. 2012, 134, 16925−16928

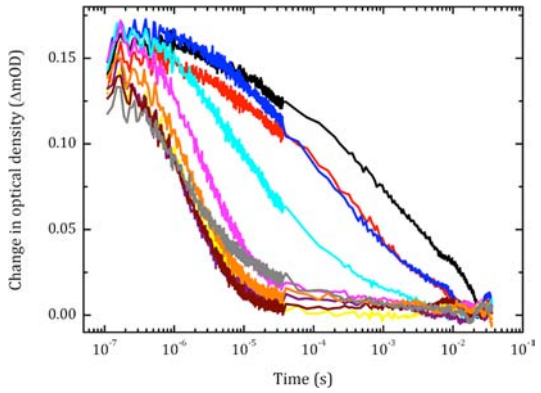

Figure 2. Changes in OD measured by TAS (setup A) for MK1-sensitized TiO_2 films in the absence of a ferrocene derivative (black) and in the presence of Br_2Fc (red), BrFc (blue), $(Me_2Si)_2Fc$ (cyan), Fc (pink), EtFc (yellow), Me_2Fc (purple), Et_2Fc (wine), iPr_2Fc (orange), and $Me_{10}Fc$ (gray), each 5 mM in benzonitrile containing 0.1 M Bu_4NPF_6. Laser excitation wavelength, 532 nm; pulse energy, 3 μJ cm^{-2}; repetition rate, 10 Hz; probe beam wavelength, 900 nm. Data were averaged from 1536 laser shots.

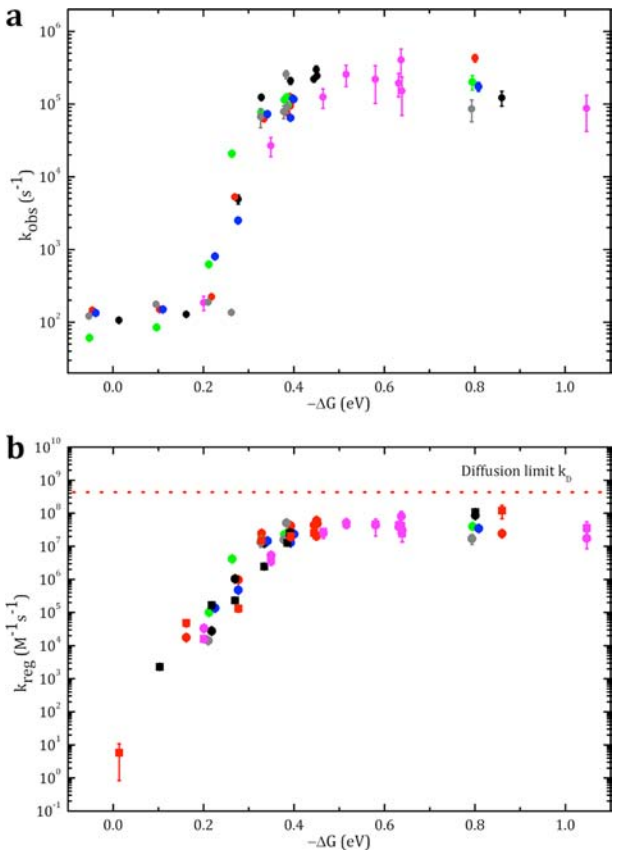

Figure 3. Dependence of (a) k_{obs} and (b) k_{reg} on $-\Delta G$ for MK1 (red), MK2 (black), MK24 (green), MK51 (blue), MK75 (pink), and MK78 (gray). Circles and squares represent data measured with TAS setups A and B, respectively. Error bars indicate uncertainties of the fit. The diffusion-limited rate constant in (b) was calculated using eq 9 for the reaction between MK1 and Fc.

The dependence of k_{obs} on the driving force $-\Delta G$ is plotted in Figure 3a. For driving forces above 19 kJ mol^{-1} (ΔE = 0.20 V), k_{reg} could be calculated from the data. For smaller driving forces, k_{obs} was constant, preventing the determination of k_{reg} since $k_{obs} \approx k_{rec2}$. k_{reg} would be smaller than 10^4 M^{-1} s^{-1}, the detection limit at the chosen concentration of the ferrocene derivatives.

The rate constants measured for various concentrations of the ferrocene derivative should yield the same rate constant in order for the data measured at lower concentrations to be related to the actual devices containing high concentrations of the redox couple. Measurements of the regeneration rate between ferrocene and MK2 for ferrocene concentrations of 2.5−100 mM resulted in consistent k_{reg} values of $(0.4–2) \times 10^5$ M^{-1} s^{-1}; similar variations are evident in the data presented in Figure 3b. As a consequence, increasing the ferrocene derivative concentration allows k_{reg} to be determined for reactions involving small driving forces for dye regeneration.

Figure 3b shows the dependence of k_{reg} on $-\Delta G$. k_{reg} increased sharply with driving force up to 29 kJ mol^{-1} (ΔE = 0.35 V), showing behavior typical for the Marcus normal region.[16] A driving force of 20−25 kJ mol^{-1} ($\Delta E \approx$ 0.20−0.25 V) was calculated from eq 7 to be sufficient to give a quantitative theoretical dye regeneration yield of Φ = 99.9% for a typical concentration of the ferrocene derivative used in DSC electrolytes (0.1 M).[6a,12] In practice, the achieved yields may differ because the structure of the film and dye aggregation could render a certain fraction of the dye molecules inaccessible, causing them to be regenerated more slowly or not at all. This effect is expected to be independent of the driving force. Furthermore, the measurements were conducted at open circuit rather than at the maximum-power point, where the electron density in the TiO_2 is reduced since the current is allowed to flow through an external load. Lower electron densities in the TiO_2 should slow the recombination and may lead to slightly increased regeneration yields. On the other hand, consumption of the reduced mediator close to the TiO_2 surface could result in a concentration gradient, reducing the regeneration yield, when current flow through an external circuit is allowed. The latter, however, is unlikely to be significant due to the usual vast excess of reduced mediator.

$$\Phi = \left(1 - \frac{k_{rec2}}{k_{reg}[Fc^{deriv}] + k_{rec2}}\right) \times 100\% \quad (7)$$

For driving forces of 29−101 kJ mol^{-1} (ΔE = 0.30−1.05 V), the dye regeneration rate was relatively constant. This surprising result indicates that dye regeneration is so rapid that the reaction rate is limited by the diffusion of the reactants toward each other.[8a] To estimate k_D, the diffusion-limited value of k_{reg}, the Smoluchowski model for diffusion-controlled reactions was modified to describe the reaction of the dye cation with the ferrocene derivative. In the Smoluchowski model, two spheres with radii r_1 and r_2 diffuse in solution with diffusion coefficients D_1 and D_2, and rapid electron transfer occurs on contact with a rate constant k_D given by eq 8.[17]

$$k_D = 4\pi(D_1 + D_2)(r_1 + r_2) \quad (8)$$

Here the dye cation cannot diffuse, as it is fixed to the titania surface. Furthermore, not all sides of the dye cation are accessible for reduction by the ferrocene derivative. Modifying eq 8 to account for this gives eq 9, which describes the reaction of a mobile sphere with an immobilized hemisphere fixed on a plane.[17] The radius of ferrocene is r_{Fc} = 4 Å.[18] Density functional theory calculations by Mori and co-workers on the dye MK3, a close structural analogue of MK1, suggested that the dyes can be described as an ellipse with $r_{x,y}$ = 4.5 Å and r_z = 10 Å.[19] If dense packing of the dye on the TiO_2 surface is

dx.doi.org/10.1021/ja3054578 | J. Am. Chem. Soc. 2012, 134, 16925−16928

assumed, the ethylcarbazole-based dye molecule can be approximated as a hemisphere with a radius of r_{dye} = 4.5 Å. These parameter values and the value of D_{Fc} from Table S1 give $k_D = 4.3 \times 10^8$ M^{-1} s^{-1} for ferrocene.

$$k_D = 2\pi D_{Fc}(r_{Fc} + r_{dye}) \quad (9)$$

Considering the approximations used in the calculation of this rate constant, it is in reasonable agreement with the average of the k_{reg} values measured in the diffusion-limited region (4.2×10^7 M^{-1} s^{-1}). The lower-than-predicted experimental value may be a result of the simplified shape of the dye, the restricted accessibility of some dye molecules due to aggregation and pore structure, and slower diffusion of the ferrocene derivatives inside the dye-sensitized mesoporous TiO_2 film. Nelson et al.[20] measured diffusion rates of a cobalt redox couple that were up to 9 times slower inside a dyed film than inside the bulk layer. Nevertheless, the calculated diffusion limit provides a useful estimate of the maximum attainable regeneration rate. Another feature of the data in Figure 3 is that the driving force determines the regeneration rate, while the structure of the dye (length of the side chains, ether groups) and the steric bulk of the redox couple appear to have only minor effects on the reaction kinetics.

In conclusion, the dependence of the dye regeneration rate constant on the driving force has been determined for a combination of six dyes and nine ferrocene derivatives. The variation in k_{reg} is in agreement with the Marcus normal region for driving forces of 0−35 kJ mol^{-1}. A driving force of 20−25 kJ mol^{-1} ($\Delta E \approx 0.20-0.25$ V) was calculated to be sufficient to achieve 99.9% theoretical dye regeneration under typical DSC operating conditions. When the driving force is increased further, the regeneration reaction becomes diffusion-controlled. The Smoluchowski model was used to estimate an upper limit for the diffusion-controlled value of k_{reg} that is in reasonable agreement with the experimental values. Structural changes in the mediator or the dye had minor effects on the regeneration rate. Future endeavors to optimize the efficiency of DSCs should aim at matching a dye with the appropriate redox couple to yield a driving force of 20−25 kJ mol^{-1}. In addition to providing guidelines on matching sensitizers with redox mediators in DSCs, the results presented here may also have implications for other photoelectrochemical devices where charge transfer processes are important.

■ ASSOCIATED CONTENT

Ⓢ Supporting Information

Experimental procedures; specifications of the used materials; and further experimental data, including CV data (Tables S1 and S2), TAS spectra (Figures S1−S6), and fitted parameter values (Tables S3−S11). This material is available free of charge via the Internet at http://pubs.acs.org.

■ AUTHOR INFORMATION

Corresponding Author

udo.bach@monash.edu; leone.spiccia@monash.edu

Notes

The authors declare no competing financial interest.

■ ACKNOWLEDGMENTS

We acknowledge financial support from the Australian Research Council through the Centre of Excellence, Discovery, Australian Research Fellowship, and LIEF Programs and from the Victorian State Government Department of Primary Industry (SERD Program, Victorian Organic Solar Cells Consortium) and Victoria's Science Agenda (VSA).

■ REFERENCES

(1) (a) O'Regan, B.; Grätzel, M. *Nature* **1991**, *353*, 737. (b) Hagfeldt, A.; Boschloo, G.; Sun, L.; Kloo, L.; Pettersson, H. *Chem. Rev.* **2010**, *110*, 6595.

(2) Daeneke, T.; Mozer, A. J.; Kwon, T.-H.; Duffy, N. W.; Holmes, A. B.; Bach, U.; Spiccia, L. *Energy Environ. Sci.* **2012**, *5*, 7090.

(3) Abbreviations for Fc derivatives: $Me_{10}Fc$, decamethylferrocene; Me_2Fc, 1,1′-dimethylferrocene; Et_2Fc, 1,1′-diethylferrocene; iPr_2Fc, 1,1′-diisopropylferrocene; EtFc, ethylferrocene; $(Me_2Si)_2Fc$, 1,1′-bis(dimethylsilyl)ferrocene; BrFc, bromoferrocene; Br_2Fc, 1,1′-dibromoferrocene. The use of acetylferrocene was also explored but not further pursued due to the light sensitivity of this compound and the decomposition of its oxidation product, acetylferrocenium, within short time frames.

(4) (a) Pavlishchuk, V. V.; Addison, A. W. *Inorg. Chim. Acta* **2000**, *298*, 97. (b) Noviandri, I.; Brown, K. N.; Fleming, D. S.; Gulyas, P. T.; Lay, P. A.; Masters, A. F.; Phillips, L. *J. Phys. Chem. B* **1999**, *103*, 6713.

(5) (a) Yu, Q.; Wang, Y.; Yi, Z.; Zu, N.; Zhang, J.; Zhang, M.; Wang, P. *ACS Nano* **2010**, *4*, 6032. (b) Boschloo, G.; Hagfeldt, A. *Acc. Chem. Res.* **2009**, *42*, 1819.

(6) (a) Daeneke, T.; Kwon, T.-H.; Holmes, A. B.; Duffy, N. W.; Bach, U.; Spiccia, L. *Nat. Chem.* **2011**, *3*, 213. (b) Feldt, S. M.; Gibson, E. A.; Gabrielsson, E.; Sun, L.; Boschloo, G.; Hagfeldt, A. *J. Am. Chem. Soc.* **2010**, *132*, 16714. (c) Bai, Y.; Yu, Q.; Cai, N.; Wang, Y.; Zhang, M.; Wang, P. *Chem. Commun.* **2011**, *47*, 4376. (d) Wang, M.; Chamberland, N.; Breau, L.; Moser, J.-E.; Humphry-Baker, R.; Marsan, B.; Zakeeruddin, S. M.; Grätzel, M. *Nat. Chem.* **2010**, *2*, 385. (e) Daeneke, T.; Uemura, Y.; Duffy, N. W.; Mozer, A. J.; Koumura, N.; Bach, U.; Spiccia, L. *Adv. Mater.* **2012**, *24*, 1222.

(7) Yella, A.; Lee, H.-W.; Tsao, H. N.; Yi, C.; Chandiran, A. K.; Nazeeruddin, M. K.; Diau, E. W.-G.; Yeh, C.-Y.; Zakeeruddin, S. M.; Grätzel, M. *Science* **2011**, *334*, 629.

(8) (a) Miller, J. R.; Beitz, J. V.; Huddleston, R. K. *J. Am. Chem. Soc.* **1984**, *106*, 5057. (b) Miller, J. R.; Calcaterra, L. T.; Closs, G. L. *J. Am. Chem. Soc.* **1984**, *106*, 3047.

(9) Rowley, J. G.; Farnum, B. H.; Ardo, S.; Meyer, G. J. *J. Phys. Chem. Lett.* **2010**, *1*, 3132.

(10) Clifford, J. N.; Palomares, E.; Nazeeruddin, M. K.; Grätzel, M.; Durrant, J. R. *J. Phys. Chem. C* **2007**, *111*, 6561.

(11) (a) Oskam, G.; Bergeron, B. V.; Meyer, G. J.; Searson, P. C. *J. Phys. Chem. B* **2001**, *105*, 6867. (b) Liu, Y.; Jennings, J. R.; Parameswaran, M.; Wang, Q. *Energy Environ. Sci.* **2011**, *4*, 564.

(12) Feldt, S. M.; Wang, G.; Boschloo, G.; Hagfeldt, A. *J. Phys. Chem. C* **2011**, *115*, 21500.

(13) (a) Anderson, A. Y.; Barnes, P. R. F.; Durrant, J. R.; O'Regan, B. C. *J. Phys. Chem. C* **2011**, *115*, 2439. (b) Mozer, A. J.; Panda, D. K.; Gambhir, S.; Winther-Jensen, B.; Wallace, G. G. *J. Am. Chem. Soc.* **2010**, *132*, 9543.

(14) (a) Ardo, S.; Sun, Y.; Staniszewski, A.; Castellano, F. N.; Meyer, G. J. *J. Am. Chem. Soc.* **2010**, *132*, 6696. (b) Cappel, U. B.; Feldt, S. M.; Schoeneboom, J.; Hagfeldt, A.; Boschloo, G. *J. Am. Chem. Soc.* **2010**, *132*, 9096.

(15) Zhang, X.-H.; Cui, Y.; Katoh, R.; Koumura, N.; Hara, K. *J. Phys. Chem. C* **2010**, *114*, 18283.

(16) Sutin, N. *Prog. Inorg. Chem.* **1983**, *30*, 441.

(17) Shoup, D.; Lipari, G.; Szabo, A. *Biophys. J.* **1981**, *36*, 697.

(18) Kirchner, K.; Dang, S. Q.; Stebler, M.; Dodgen, H. W.; Wherland, S.; Hunt, J. P. *Inorg. Chem.* **1989**, *28*, 3604.

(19) Miyashita, M.; Sunahara, K.; Nishikawa, T.; Uemura, Y.; Koumura, N.; Hara, K.; Mori, A.; Abe, T.; Suzuki, E.; Mori, S. *J. Am. Chem. Soc.* **2008**, *130*, 17874.

(20) Nelson, J. J.; Amick, T. J.; Elliott, C. M. *J. Phys. Chem. C* **2008**, *112*, 18255.